ELSEVIER

Tectonophysics 349 (2002) 251–275

TECTONOPHYSICS

www.elsevier.com/locate/tecto

The thermal history of the eastern Officer Basin (South Australia): evidence from apatite fission track analysis and organic maturity data

Peter R. Tingate [a,*], Ian R. Duddy [b,1]

[a] *National Centre for Petroleum Geology and Geophysics, University of Adelaide, Adelaide, South Australia 5005, Australia*
[b] *Geotrack International Pty. Ltd., 37 Melville Road, Brunswick West, Victoria 3055, Australia*

Received 3 November 2000; accepted 27 July 2001

Abstract

The eastern Officer Basin in South Australia contains a Neoproterozoic to Devonian succession overlain by relatively thin (< 500 m) Permian, Mesozoic and Tertiary deposits. Within the basin fill, there are several major unconformities representing uncertain amounts of erosion. Three of these surfaces are associated with regional deformational events. Regional unconformities formed between 560 and 540 Ma (Petermann Ranges Orogeny), approximately 510–490 Ma (Delamerian Orogeny), 370–300 Ma (Alice Springs Orogeny), 260–150 Ma; and 95–40 Ma. AFTA® results from 13 samples of Neoproterozoic, Cambrian and Permian sedimentary rocks in five wells (Giles-1, Manya-2, -5 and -6 and Lake Maurice West-1) show clear evidence for a number of distinct thermal episodes. Results from all samples are consistent with cooling from the most recent thermal episode beginning at some time between 70 and 20 Ma (Maastrichtian–Miocene). AFTA results from Giles-1 indicate at least two pre-Cretaceous thermal episodes with cooling beginning between 350 and 250 Ma (Carboniferous–Permian) and between 210 and 110 Ma (Late Triassic–Albian). Results from Manya-2, -5 and -6 and Lake Maurice West-1 show evidence for at least one earlier higher temperature event, with cooling from elevated paleotemperatures beginning between 270 and 200 Ma (Late Permian to Late Triassic). These episodes can be correlated with other cooling/erosional events outside the study area, and the AFTA-derived paleotemperatures are consistent with kilometre-scale erosion for each of the episodes identified. Integration of the AFTA data with organic thermal maturation indicators (MPI) in the Manya and Giles-1 wells suggests that the Cambrian and Neoproterozoic successions in the northern part of the study area reached peak maturation prior to the Permian, while limited data from Lake Maurice West-1 allows peak maturation to have occurred as young as the Late Permian to Late Triassic thermal episode revealed by AFTA. The approach outlined in this study is relevant to all ancient basins as it emphasises the importance of understanding events associated with neighbouring regions. The thermal history of the Officer Basin, as with most other ancient basins, has been strongly affected by significant tectonic events throughout its history, even though younger deposits are not preserved in the basin itself. The recognition of these younger events, and the implications of these events for the depositional history, is important as it allows identification of the best regions for preservation of early generated hydrocarbons, and in some cases, suggests areas where generation of hydrocarbons could have occurred more recently than previously thought.

Keywords: AFTA; Fission track; Officer Basin; Thermal history; Hydrocarbon prospectivity

* Corresponding author. Fax: +61-8-8303-4345.
E-mail addresses: ptingate@ncpgg.adelaide.edu.au (P.R. Tingate), mail@geotrack.com.au (I.R. Duddy).
[1] Fax: +61-3-9380-1477.

0040-1951/02/$ - see front matter
PII: S0040-1951(02)00056-2

1. Introduction

The Officer Basin is a relatively unexplored region in southern central Australia with some oil shows (Fig. 1) but no economic hydrocarbon accumulations (O'Neil, 1997). The basin contains Neoproterozoic–Paleozoic sedimentary rocks separated by regional unconformities that represent uncertain amounts of erosion. These surfaces range from the latest Neoproterozoic to mid-Paleozoic in age. Overlying the Officer Basin are thin (< 500 m) Permian (Arckaringa Basin), Cretaceous (Eromanga Basin) and Tertiary successions, also separated by unconformities.

Due to the pre-Devonian age of much of the Officer Basin, true vitrinite is restricted to relatively minor occurrences in limited well intersections of Permian and Mesozoic sediments. As a result, AFTA® (Geotrack, 1994; Tingate, 1994) and organic maturation

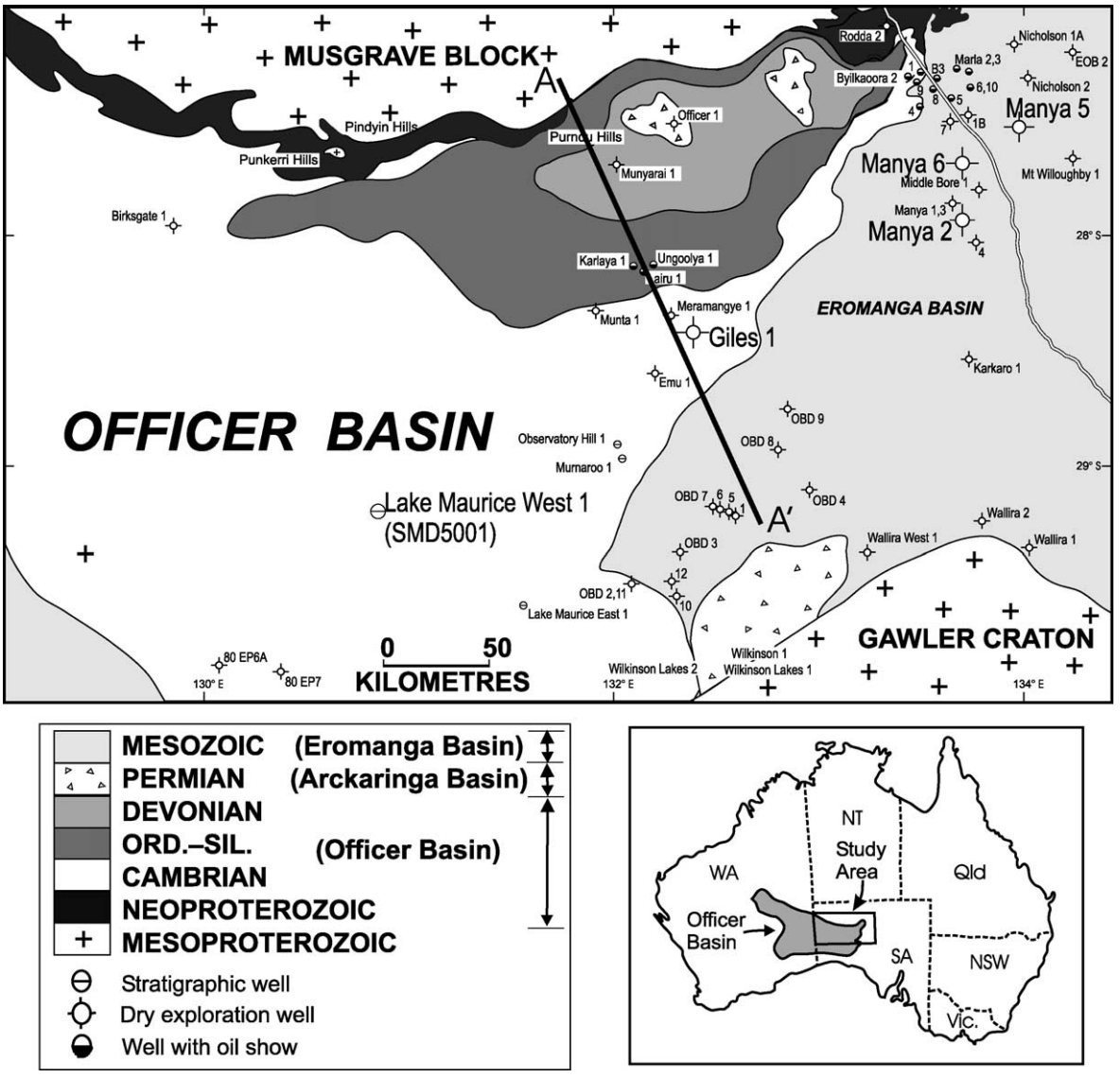

Fig. 1. Pre-Tertiary subcrop geological map of the Officer Basin (modified after Morton, 1997). A–A′ shows the line of section in Fig. 3.

studies (McKirdy and Michaelsen, 1994) were commissioned by Mines and Energy South Australia to help constrain the thermal history of the region and the timing of petroleum generation. The thermal history may also be useful in helping understand its geological development from part of a continent-scale intracratonic sag to a smaller structurally controlled basin (Hoskins and Lemon, 1995; Lindsay and Leven, 1996).

The AFTA data were originally collected and interpreted without accompanying apatite chemical compositions (Geotrack, 1994; Tingate, 1994; Gravestock and Hill, 1997; Tingate and Duddy, 2000). In this study, chlorine has been determined in all apatite grains in which ages and track lengths were measured and the AFTA data reinterpreted using a multi-compositional kinetic description of apatite annealing that provides estimates of paleotemperatures and time at $\pm$ 95% confidence limits (Green et al., 1996). Since the apatites display variation in chemical composition within and between samples the resulting thermal history has been significantly revised, illustrating the importance of incorporating the chemistry of analysed apatites into the thermal history interpretation of fission track data.

2. Regional geology

The Officer Basin is an intracratonic basin located in South and Western Australia, covering an area of approximately 350,000 km^2 (Fig. 1) and containing up to 10 km of Neoproterozoic to Late Devonian sedimentary rocks (Fig. 2). The eastern part of the Officer Basin is bounded by crystalline basement: to the north by the Musgrave Block, to the southeast by the Gawler Craton and to the south by the Coompana Block.

The Officer Basin succession contains shallow marine, aeolian, fluvial, lacustrine and glacial deposits (Fig. 2). Gravestock (1997) sub-divided the regional depositional history into 11 sequences (Fig. 2). For further stratigraphic information, the reader is referred to Moussavi-Harami and Gravestock (1995) and Morton (1997).

Hoskins and Lemon (1995) have summarised the development of the eastern Officer Basin into four stages (Fig. 3). Stage 1 consists of the initiation of the Officer Basin as part of a larger sag basin, termed the Centralian Superbasin (Walter et al., 1995) that covered much of Australia. This basin phase culminated in minor erosion at 780 to 760 Ma. Stage 2 consists of deposition within a N–S compressional basin building to the Petermann Ranges Orogeny in the latest Neoproterozoic (560 to 545 Ma) with significant N–S shortening-induced folding and thrusting (Figs. 2 and 3). Stage 3 consists of renewed sedimentation followed by another deformational event, the Delamerian Orogeny (510 to 490 Ma). At this time, further thrusting occurred and reactivated Stage 2 structures. Stage 4 consists of Ordovician to Devonian sedimentation ending again in N–S shortening associated with the Alice Springs Orogeny (370 to 300 Ma). Reactivation of older thrusts also occurred in this event, with most of the deformation probably occurring in the late Devonian to mid-Carboniferous (360 to 320 Ma), by analogy with the Amadeus Basin (Shaw, 1991).

The eastern Officer Basin contains all the required petroleum system elements (Magoon and Dow, 1994) but large uncertainty exists as to the timing of hydrocarbon. Hoskins and Lemon (1995) not only suggested that the Petermann Ranges Orogeny (560 to 545 Ma) was the major control on existing basin morphology but also concluded that the Petermann Ranges, Delamerian and Alice Springs Orogenies were all capable of causing structural traps and placing source rocks in the oil window. Gravestock and Hill (1997) produced burial history models suggesting that the three events listed above differed in importance depending on the location in the basin.

3. Thermal history reconstruction methodology

3.1. AFTA data

The interpretation of the thermal history from AFTA data in this study is based upon the annealing behaviour of spontaneous fission tracks in geological environments (Gleadow et al., 1983; Green et al., 1989a) and length data from geological samples (Gleadow et al., 1986), together with descriptions of induced fission track annealing in laboratory experiments (Green et al., 1986; Laslett et al., 1987; Duddy et al., 1988) that have been extended to geological situations (Green et al., 1989b). The laboratory annealing studies have concentrated on fission track

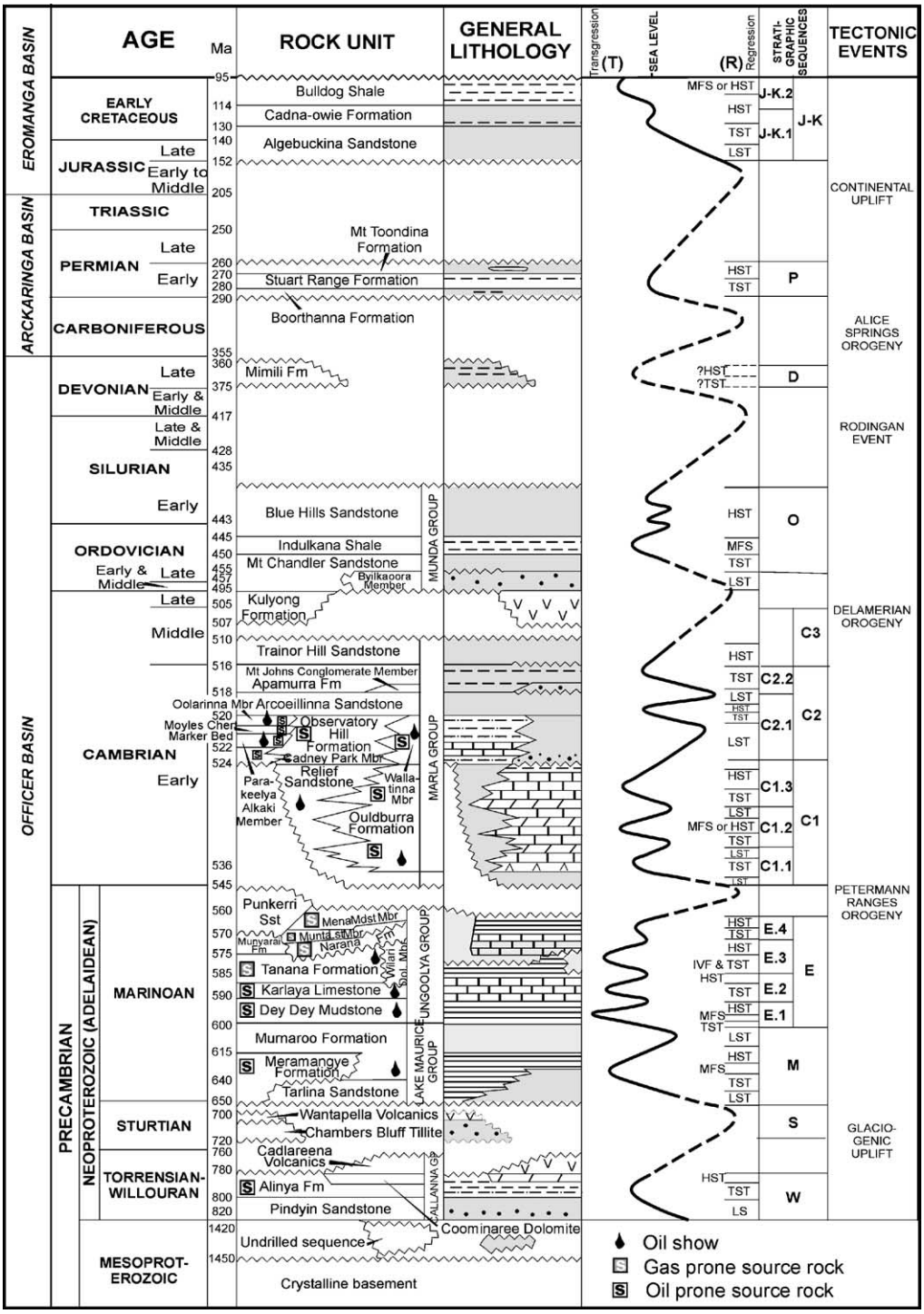

Fig. 2. Stratigraphic column for the Officer Basin and cover successions (modified after Gravestock and Morton, 1997). Stratigraphic sequences and relative sea-level information comes from Gravestock (1997).

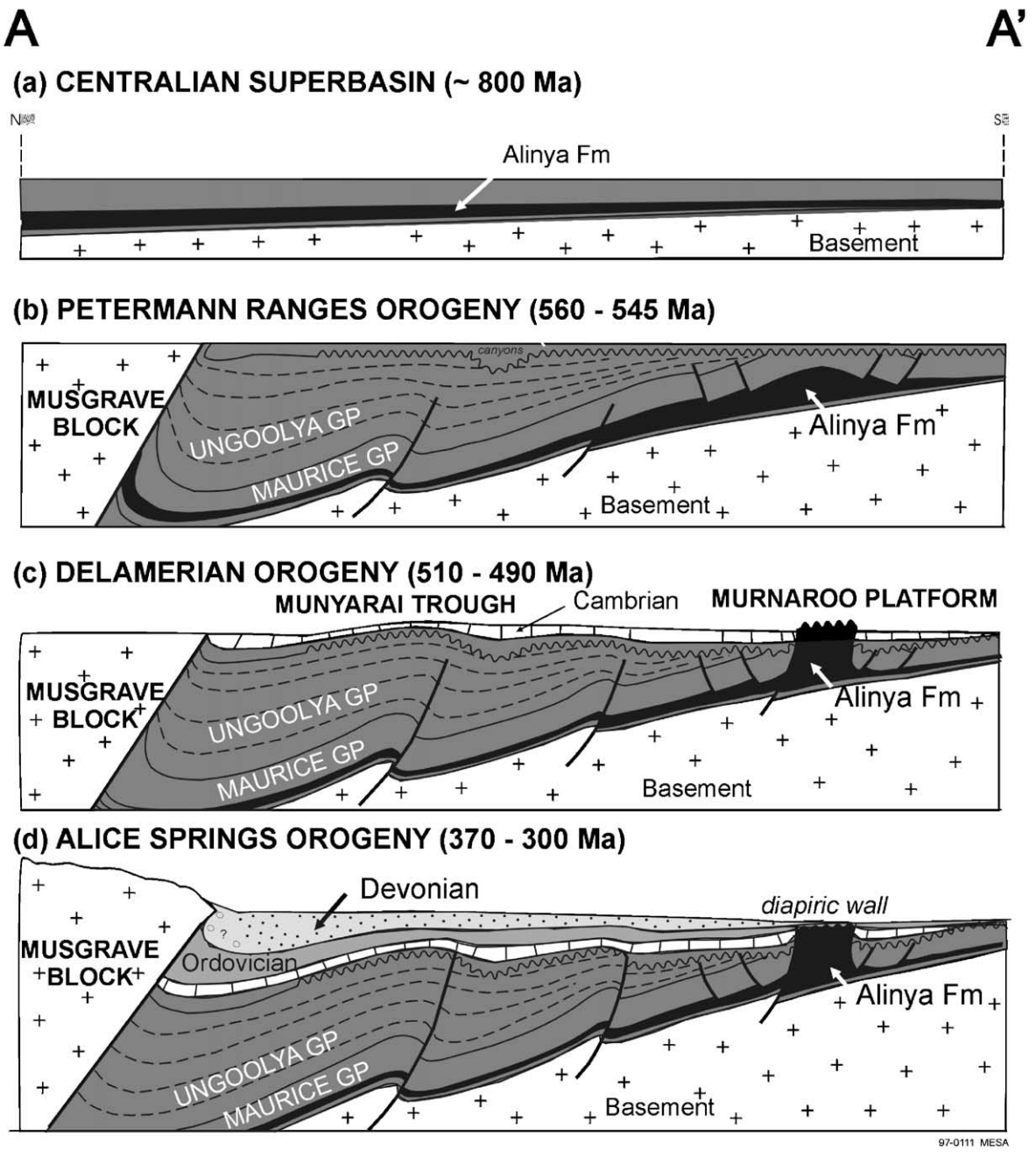

Fig. 3. Schematic Precambrian to Carboniferous history, Officer Basin (modified after Hoskins and Lemon, 1995).

length measurements and their relation to fission track density (and hence age) and have been described by Laslett et al. (1984) and Green (1988). Information on the effect of apatite chemical composition on track annealing comes from Green et al. (1985, 1986, 1996), Sieber (1986) and Tingate (1990).

The measured fission track age and track length data for each well sample were grouped based on the

chlorine content of each apatite grain in which ages and lengths were measured. Interpretation proceeded by assessing whether the fission track age and track length parameters determined for each chlorine compositional group in each sample could have been produced if the sample has never been hotter than its present temperature at any time since deposition. To make this assessment, a ''Default Thermal History'' was defined for each sample, derived from the preserved sedimentary section in the well and assuming no erosion occurred within the sedimentary succession, combined with constant values for paleogeothermal gradient and paleo-surface temperature which are adopted from present-day values. The AFTA parameters expected on the basis of this Default Thermal History were then predicted using a multi-compositional kinetic model for fission track annealing in apatite as described by Green et al. (1996).

If the measured AFTA data show a greater degree of fission track annealing (in terms of either fission track age reduction or track length reduction) than expected on the basis of this history, the sample must have been hotter at some time in the past. In this case, the AFTA data are analysed to provide estimates of the magnitude of the maximum paleotemperature in that sample, and the timing of cooling from the thermal maximum.

As AFTA data provide no information on the approach to a thermal maximum, they cannot independently constrain the heating rate and a value must therefore be assumed in order to interpret the data. The resulting paleotemperature estimates are therefore conditional on this assumed value. AFTA data can provide good control on the history after cooling from maximum paleotemperatures through the lengths of tracks formed during this period (e.g. Green et al., 1989b). On this basis, data from each sample are interpreted here in terms of two episodes of heating and cooling, as the inherent spread of the track length data is such that it is usually not possible to reveal more than one additional episode between the thermal maximum and the present-day. In this study, heating and cooling rates of 1 °C/Ma for heating and 10 °C/Ma for cooling have been assumed during each episode.

The timing of the onset of cooling and the peak paleotemperatures during the two episodes are varied systematically using a forward modelling approach, and by comparing predicted and measured parameters the range of temperature–time conditions, which are compatible with the data within $\pm$95% confidence limits can be defined. Thus for each sample, we define the time and temperature conditions of the two dominant thermal episodes required to explain the measured data. In cases where a sample actually has been subjected to more than two thermal episodes, the maximum temperature episode and the most recent episode are the two episodes defined in our approach, and no formal quantitative constraints can be placed on the intervening episode from the AFTA results alone. However, integration of results from individual samples in a vertical depth section, can allow such intermediate thermal events to be revealed and quantified to provide a more complete quantitative description of the thermal history as in the approach taken here.

More detail regarding the methods used in this study is given in Gibson and Stuwe (2000). From the interpretation of the fission track data, constraints can be placed upon the thermal history, and for most situations a number of different thermal histories can be constructed from these constraints. The choice of a particular style of thermal history for a region is a matter of geological interpretation.

3.2. Vitrinite reflectance equivalent data

Where present, vitrinite reflectance or vitrinite reflectance equivalent (VRE) data were converted to a maximum paleotemperature using the EasyRo algorithm of Burnham and Sweeney (1989). The paleotemperature obtained was calculated assuming 1 °C/Ma for heating and 10 °C/Ma for cooling. VRE data were selected from those compiled in Gravestock and Hill (1997). The major source of the VRE information was methylphenanthrene Index (MPI) data produced by McKirdy and Michaelsen (1994) and Kamali (1995). Only values derived from core samples without oil staining using the calculation method of Radke and Welte (1983) were used for thermal history analysis. The other source of VRE data was fluorescence alteration of multiple macerals (FAMM) (Michaelsen et al., 1997; Wilkins et al., 1994). Some Officer Basin Rock Eval data is also presented in Gravestock and Morton (1997) for Giles-1 and Manya-6. Rock Eval T_{max} data was not used for setting maturity levels as they are commonly

influenced by both thermal history and organic matter type (Sherwood and Russell, 1996). In Manya-6, the values appear to be low, related to the organic matter type and a mineral matrix effect (McKirdy et al., 1984).

4. Thermal history results

4.1. Sample details

Fourteen samples were collected from core for processing and thirteen provided sufficient apatite for AFTA, with apatite yields ranging from fair to mostly excellent (Table 1). Most apatite grains range from sub-rounded to very rounded in shape with anhedral grains dominant in samples GC531-3 and -6 (Cadney Park Formation and Relief Sandstone, respectively), while euhedral grains were found in sample GC531-7 (Murnaroo Fm). The numerical AFTA data are generally regarded as of excellent quality with the majority of samples providing the target 20 grains for age determination and 100 confined track length measurements (Table 2). These data form the basis for reliable thermal history interpretations.

4.2. Present temperatures

In application of any technique involving estimation of paleotemperatures, it is critical to control the present temperature profile since estimation of maximum paleotemperatures proceeds from trying to determine how much of the observed effect could be explained by the magnitude of present temperatures. Unfortunately, no temperature data were available for the wells analysed in this study and only two present-day geothermal gradient estimates are available from the South Australian portion of the basin as a whole: 14 and 24 °C/km (Gravestock and Hill, 1997). For this study, a present-day geothermal gradient of 25 °C/km has been assumed for all wells, and this has been combined with a present-day surface temperature of 25 °C in calculating the current temperature of each AFTA sample. While this assumption introduces some uncertainty into the thermal history reconstruction, the

Table 1
Sample data, eastern Officer Basin

Sample number	Depth (m)	Formation	Stratigraphic age (Ma)	Apatite yield	Present temperature (°C)[a]
Manya-2					
GC531-1	245.5–247.7	Mt Toondina Fm	270–260	poor	31
GC531-2	492.9–494.3	Boorthanna Fm	290–280	excellent	37
GC531-3	510–516	Cadney Park Fm	524–522	excellent	38
Manya-6					
GC531-4	448.2–448.8	Cadney Park Fm	524–522	good	36
GC531-5	1699.6–1701.2	Relief Sst	545–524	excellent	68
Manya-5					
GC531-6	455.1–455.5	Relief Sst	545–524	excellent	36
GC531-7	459–459.6	Murnaroo Fm	640–600	excellent	37
GC531-8	1054.5–1055.8	Tarlina Sst	650–640	excellent	51
Lake Maurice West-1(SMD 5001)					
GC531-9	217.7–218.7	Relief Sst	545–524	excellent	30
GC531-10	488.2–488.8	Murnaroo Fm	640–600	excellent	37
Giles-1					
GC531-11	416.6–416.9	Relief Sst	545–524	excellent	35
C531-12	422.3–422.6	Tanana Fm	585–575	excellent	36
GC531-13	1063.4–1063.8	Meramangye Fm	640–615	excellent	51

[a] Present temperature calculated assuming a current surface temperature of 25 °C and a geothermal gradient of 25 °C/km.

Table 2
Apatite fission track analytical results

Sample no. and well	No. of grains	Rho D $\times 10^6$ (ND)	Rho S $\times 10^6$ (Ns)	Rho I $\times 10^6$ (Ni)	U (ppm)	$P(\chi^2)$ (%)	Age dispersion (%)	Fission track age (Ma)	Mean track length (μm)	S.D. (μm)	No. of tracks
Manya-2											
GC531-1	9	1.300 (1991)	2.797 (264)	3.496 (330)	31	41	2	201.2 ± 17.6	11.59 ± 0.34	1.47	19
GC531-2	20	1.295 (1991)	2.871 (840)	2.560 (749)	23	16	12	279.2 ± 16.2	11.76 ± 0.15	1.54	106
GC531-3	20	1.290 (1991)	1.825 (472)	1.914 (495)	17	11	21	237.2 ± 16.8	11.35 ± 0.25	2.57	105
Manya-6											
GC531-4	20	1.284 (1991)	3.095 (1188)	3.246 (1246)	29	7	2	236.2 ± 11.8	11.43 ± 0.19	1.70	76
GC531-5	15	1.279 (1991)	1.662 (449)	1.776 (533)	16	< 1	36	231.0 ± 15.9 *218.8 ± 26.9*	11.21 ± 0.64	2.92	21
Manya-5											
GC531-6	20	1.274 (1991)	1.803 (523)	2.048 (594)	18	58	3	216.6 ± 14.5	11.92 ± 0.15	1.57	104
GC531-7	20	1.268 (1991)	1.718 (468)	2.195 (598)	20	< 1	29	192.1 ± 13.1 *195.6 ± 20.8*	12.22 ± 0.28	2.00	52
GC531-8	20	1.263 (1991)	0.683 (375)	0.697 (383)	6	26	18	238.4 ± 18.7	11.23 ± 0.21	2.12	102
LM west-1											
GC531-9	20	1.257 (1991)	3.812 (806)	2.838 (600)	26	60	< 1	323.6 ± 19.9	12.12 ± 0.22	2.32	108
GC531-10	20	1.252 (1991)	2.918 (762)	2.933 (766)	27	66	3	240.2 ± 14.2	11.98 ± 0.16	1.68	106
Giles-1											
GC531-11	20	1.247 (1991)	3.384 (888)	2.706 (710)	25	81	3	299.3 ± 17.4	11.95 ± 0.18	1.79	102
GC531-12	20	1.241 (1991)	1.916 (704)	1.820 (669)	17	< 1	28	251.6 ± 15.5 *233.5 ± 22.3*	12.10 ± 0.18	1.74	90
GC531-13	20	1.236 (1991)	1.320 (255)	2.138 (413)	20	< 1	55	148.2 ± 12.6 *139.6 ± 22.8*	11.16 ± 0.19	1.87	100

Rho S = spontaneous track density; Rho I = induced track density; Rho D= track density in standard glass external detector.
All track densities quoted in units of 10^6 tracks per square centimeter. Brackets show number of tracks counted.
Rho D and Rho I measured in mica external detectors: Rho S measured in internal surfaces.
Italics indicate a central age — used where sample contains a significant spread of single grain ages [$P(\chi^2) < 5\%$]. Errors quoted at ± 1 sigma.
Ages calculated using dosimeter glass CN5, with a zeta of 392.9 ± 7.4. Age and track length analyst is M. Moore.

conservative choice of a value at the top end of the measured range suggests that our estimates of the net degree of cooling involved in any thermal episode will be underestimates rather than overestimates. Furthermore, all samples are from relatively shallow depths, so that the present-day temperatures of all

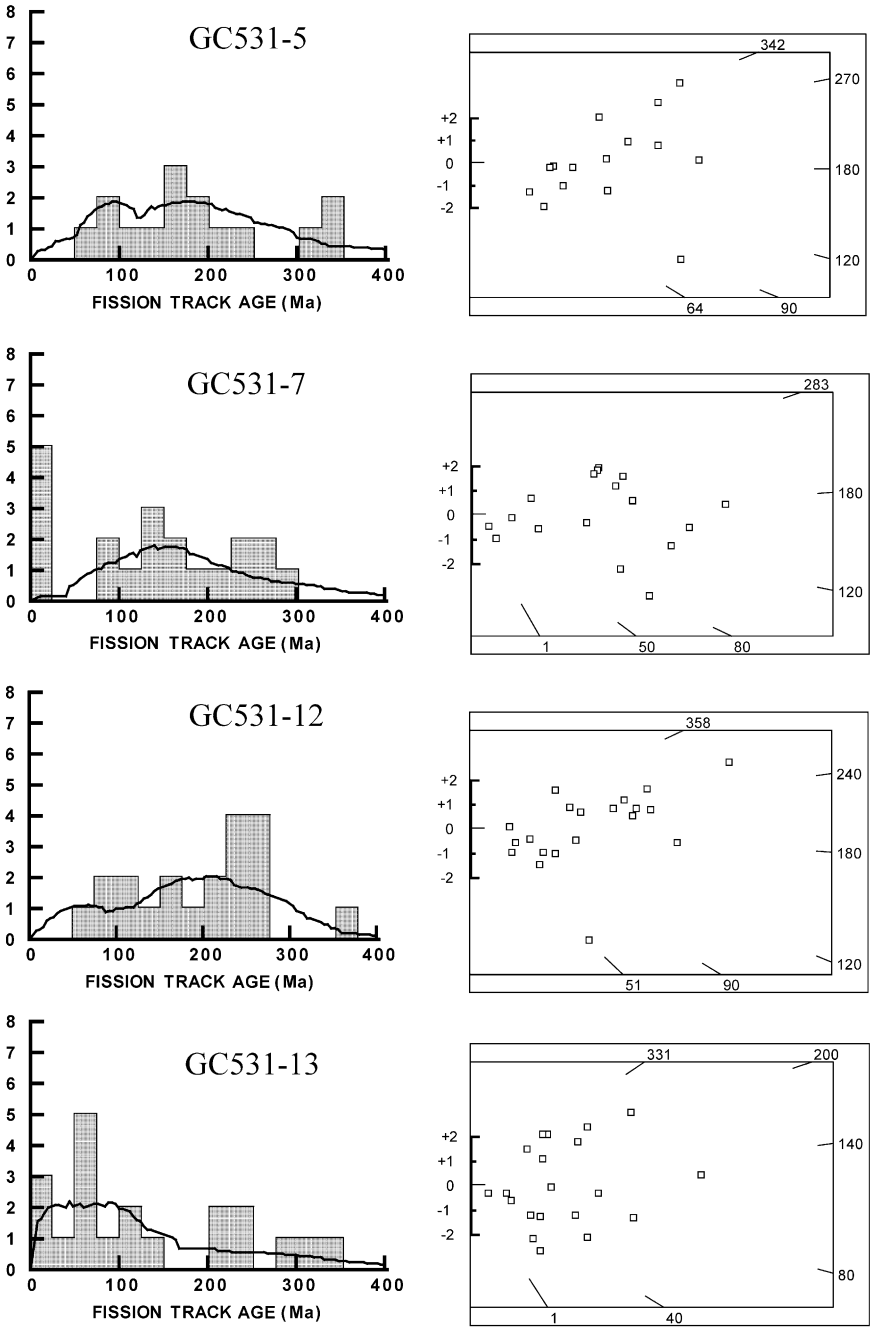

Fig. 4. Single grain age histograms and radial plots (Galbraith, 1990) for samples with $P(\chi^2) < 5\%$ (see Table 2).

samples are less than 70 °C (Table 1), at which contemporary fission track annealing is minor (e.g. Green et al., 1989a).

4.3. AFTA results

All AFTA analytical details are presented in Table 2. The mean fission track ages (pooled and central) from drilled depths less than 500-m range in age from approximately 190 to 330 Ma with a tendency for the ages to decrease generally from the southwest to the northeast. Single grain age variation in four samples (of 13) with $P(\chi^2)$ values less than 5% is illustrated in Fig. 4. The length parameters show little variation across the region (Fig. 5): mean track lengths vary between 11.2 and 12.3 μm and standard deviations are all greater than 1.5 μm.

Most samples have a very narrow range of chlorine content (0.0 to 0.2 wt.% Cl with occasional grains with up to ~ 0.5 wt.% Cl) typical of quartzose sandstones derived from granitic terrains (e.g., sample GC531-4 as shown in Fig. 6). Apatite from samples of Permian Boorthanna Formation (GC531-2) and Proterozoic Cadney Park Formation (GC531-3) from Manya-2 contain apatites with broad ranges of Cl contents, up to 2.1 wt.% in sample GC531-2 (Fig. 6), suggesting the presence of a range of volcanogenic detritus (Duddy, unpublished results; Mitchell, 1998).

4.4. AFTA thermal history interpretations

Thermal history constraints from each sample in terms of the magnitude and timing of paleotemperatures (± 95% confidence limits) are summarised in Table 3. The constraints listed in Table 3 are derived from the maximum likelihood solutions of the AFTA results in each sample for two thermal episodes. Examples of these solutions, plotted in time–temperature space, are presented in Fig. 7 for the three samples from the Giles-1 well. The solution for sample GC531-11 from the Cambrian Relief Sst (present temperature 35 °C) indicates cooling from paleotemperatures of 95 to 100 °C beginning at some time between 400 to 250 Ma, followed by cooling from 75 to 85 °C, at some time between 125 and 5 Ma. The solution for sample GC531-12 from the underlying Precambrian Tanana Formation (present temperature 36 °C) is very similar, with cooling from paleotemperatures of 100 to 105 °C beginning at some time between 350 to 200 Ma, followed by cooling from 70 to 85 °C, at some time between 110 and 10 Ma. The results from both samples would also allow an intervening thermal episode with cooling from paleotemperatures intermediate between those in the two defined episodes, as illustrated schematically by the horizontal-hatched area in Fig. 7. Support for such an intervening episode comes from the solution for the deepest Precambrian sample, GC531-13 (Meramangye Formation, present temperature 51 °C). The AFTA solution indicates cooling from 100 to 105 °C beginning between 210 and 110 Ma, followed by cooling from 85 to 90 °C between 70 and 10 Ma. Note, the AFTA results for sample GC531-13 provide no direct evidence for any part of the thermal history prior to 210 Ma because of the near total annealing of a fission tracks in the 210 to 110 Ma episode. However, higher paleotemperatures are allowed by the data at any time prior to 210 Ma, as illustrated for a notional episode described by the crosshatched area in Fig. 7. Thus, integration of the AFTA results from individual samples in this way allows a more complete picture of the post-Cambrian thermal history of the region to be built, even where younger rocks are no longer preserved.

Timing constraints at ± 95% confidence limits obtained from the maximum likelihood solutions in all AFTA samples in the five Officer Basin wells studied are illustrated by the horizontal bars in Fig. 8. Assuming that the paleo-thermal episodes identified in individual samples from a well represent pervasive, synchronous events, then the overlap in AFTA-derived timing from the individual samples can provide a better estimate of the timing of discrete events, as discussed for each well in the following section. Also shown on Fig. 8 are the time ranges of major regional unconformities: 560 to 540 Ma (Petermann Ranges Orogeny); ~ 510–490 Ma (Delamerian Orogeny); 370–300 Ma (Alice Springs Orogeny), 260–150 Ma; and 95–40 Ma, with which the timing constraints from individual samples may be compared.

4.4.1. Giles-1

Thermal history solutions for the Giles-1 samples have been described in detail above and are shown in Fig. 7. In summary, at least two, but possibly more, thermal episodes are required by the AFTA data in the

single Cambrian (GC531-11) and two Neoproterozoic samples (GC531-12 and -13) analysed. At least one post-Early Cretaceous (< 110 Ma) thermal episode is required in the deepest Neoproterozoic Meramangye Fm sample (GC531-13) with cooling from peak paleotemperatures of 85 to 95 °C beginning at some time between 70 and 10 Ma (Maastrichtian to Late Miocene). Results from the two shallower samples are consistent with a similar magnitude of cooling beginning during that same time interval, but also allow cooling to have begun somewhat earlier; between 125 and 10 Ma in sample GC531-11 and between 110 and 10 Ma in sample GC531-12 (Fig. 8). It is possible that cooling occurred in a number of discrete episodes

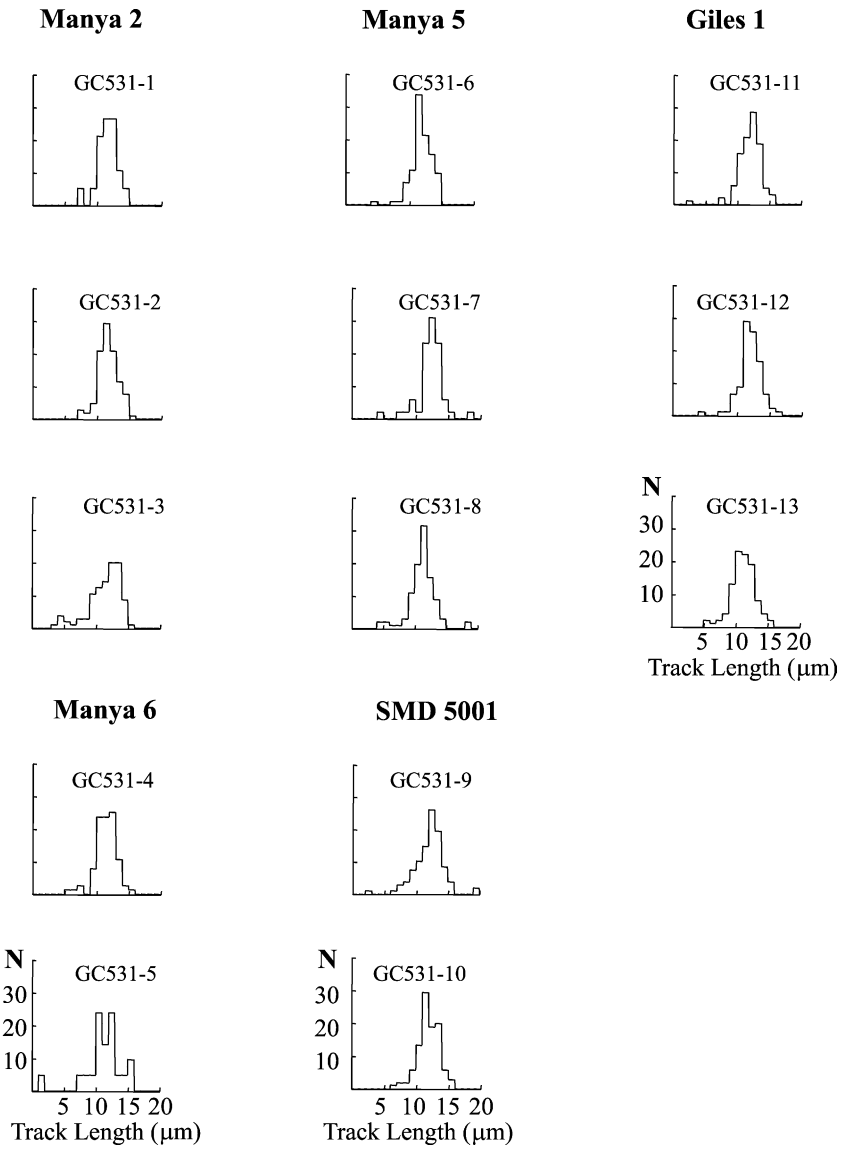

Fig. 5. Confined track length distributions for all samples in Table 2. All track length distributions are normalised to 100 tracks.

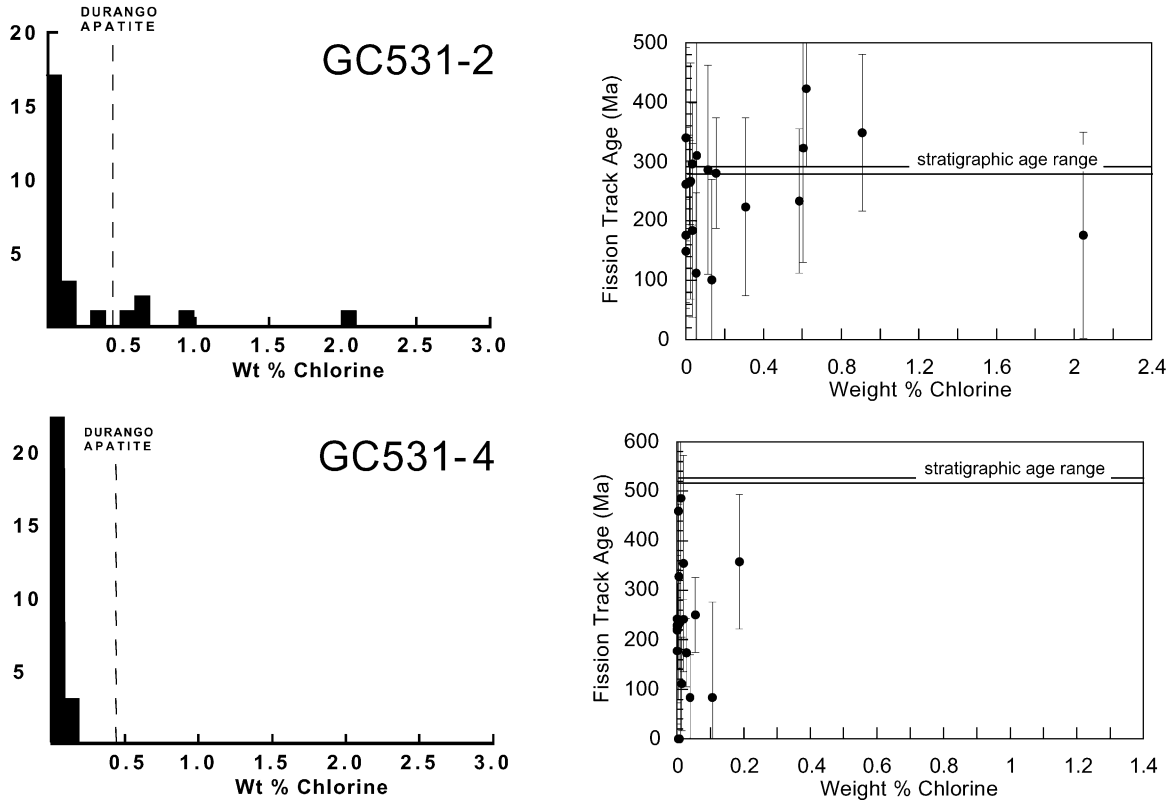

Fig. 6. Chlorine content histograms and plots of fission track age versus chlorine content for samples GC531-2 and GC531-4.

beginning in the mid-Cretaceous, but the available data do not allow these episodes to be uniquely resolved.

The AFTA results from Giles-1 also require at least two, and possibly more, pre-Albian (>110 Ma) thermal episodes (Table 3; Figs. 7 and 8). Timing constraints from the closely spaced samples GC531-11 and -12 display the largest overlap, consistent with cooling from ~100 °C beginning at some time between 350 and 250 Ma (Carboniferous–Permian). Results from sample GC531-13 indicate a distinctly younger thermal episode, with cooling from a similar paleotemperature (~ 100 to 105 °C) not occurring until 210 to 110 Ma (Late Triassic to Albian). As illustrated schematically in Fig. 7, the AFTA results in this sample would allow an earlier thermal episode involving paleotemperatures >105 °C between 350 and 250 Ma, as required by AFTA in the shallower samples.

Analysis of timing overlaps in this well does not provide unique constraints, but although there is some uncertainty in the precise timing of the thermal episodes revealed by AFTA, the occurrence of at least two thermal episodes prior to the Albian is clear.

4.4.2. Lake Maurice West-1

At least two, but possibly more, thermal episodes are required by the AFTA data in the two Cambrian and Precambrian samples (GC531-9 and -10) analysed from Lake Maurice West-1. In the earliest episode revealed by AFTA, overlapping timing constraints suggest that both samples began to cool at some time between 310 and 190 Ma (Late Carboniferous to Early Jurassic); sample GC531-9 from 95 to 100 °C and sample GC531-10 from 100 to 105 °C. AFTA also indicates a second consistent thermal episode, with cooling beginning between 110 and 20 Ma (Albian to Early Miocene): sample GC531-9 from

Table 3
Paleotemperature analysis summary from AFTA samples from the Officer Basin, South Australia

AFTA sample number (GC-)	Stratigraphic unit	From AFTA and VR					
		Oldest episode (s)		Intermediate episode (s)		Recent episode (s)	
		Maximum paleotemperature[a] (°C)	Onset of cooling (Ma)	Maximum paleotemperature[a] (°C)	Onset of cooling (Ma)	Maximum paleotemperature[a] (°C)	Onset of cooling (Ma)
Manya-2							
531-1	Mt Toondina (245.5–247.7 m, Permian)	Not applicable		*(70–110)*	*(Post-Depn)*	<90	90 to 0
531-2	Boorthanna (492.9–494.3 m, Permian)	Not applicable		*(85–110)*	*(Depn to 80)*	60–85	70 to 0
531-3	Cadney Park (510–516 m, Cambrian)	105–110	300 to 200	*(85–105)*	*(200 to 110)*	75–90	110 to 10
Manya-6							
531-4	Cadney Park (448.2–448.8 m, Cambrian)	105–110	325 to 200	*(85–105)*	*(200 to 70)*	75–85	70 to 0
531-5	Relief Sst (1699.6–1701.2 m, Cambrian)	(95–130)	(Depn to 50)	*(95–105)*	*(350 to 50)*	<105	110 to 0
Manya-5							
531-6	Relief Sst (455.1–455.5 m, Cambrian)	100–110	300 to 190	*(85–100)*	*(190 to 90)*	75–85	90 to 15
531-7	Murnaroo (459.0–459.6 m, Precambrian)	>105	270 to 200	*(85–105)*	*(200 to 110)*	65–85	110 to 0
531-8	Tarlina Sst (1054.5–1055.8 m, Precambrian)	100–105	310 to 160	*(85–100)*	*(160 to 80)*	75–85	80 to 0
Lake Maurice West-1 (SMD 5001)							
531-9	Relief Sst (217.7–218.7 m, Cambrian)	95–100	340 to 190	*(80–95)*	*(190 to 110)*	60–80	110 to 0
531-10	Murnaroo (488.2–488.8 m, Precambrian)	100–105	310 to 190	*(85–100)*	*(190 to 110)*	75–85	110 to 20
Giles-1							
531-11	Relief Sst (416.6–416.9 m, Cambrian)	95–100	400 to 250	*(85–95)*	*(250 to 125)*	75–85	125 to 5
531-12	Tanana (422.3–422.6 m, Precambrian)	100–105	350 to 200	*(85–100)*	*(200 to 110)*	70–85	110 to 10
531-13	Meramangye (1063.4–1063.8 m, Precambrian)	*(>105)*	*(>210)*	100–105	210 to 110	85–90	70 to 10

Bracketed and italicised constraints indicate paleo-thermal episodes which are *allowed* by AFTA, but *not required*.
[a] All AFTA paleotemperature estimates are derived assuming a heating rate of 1 °C/Ma and a cooling rate of 10 °C/Ma (see text).

60 to 80 °C and sample GC531-10 from 75 to 85 °C (Table 3; Fig. 8).

4.4.3. Manya-2, Manya-5 and Manya-6

At least two, but possibly more thermal episodes are required to account for the AFTA data in the six Cambrian and Precambrian samples analysed from Manya-2 (GC531-3), Manya-5 (GC531-6, -7 and -8) and Manya-6 (GC531-4 and -5).

In the earliest episode revealed by AFTA, overlapping timing constraints suggest all samples began to cool at some time between 270 and 200 Ma (Permian to Triassic); sample GC531-3 from 105 to 110 °C (300 to 200 Ma), sample GC531-4 from 105 to

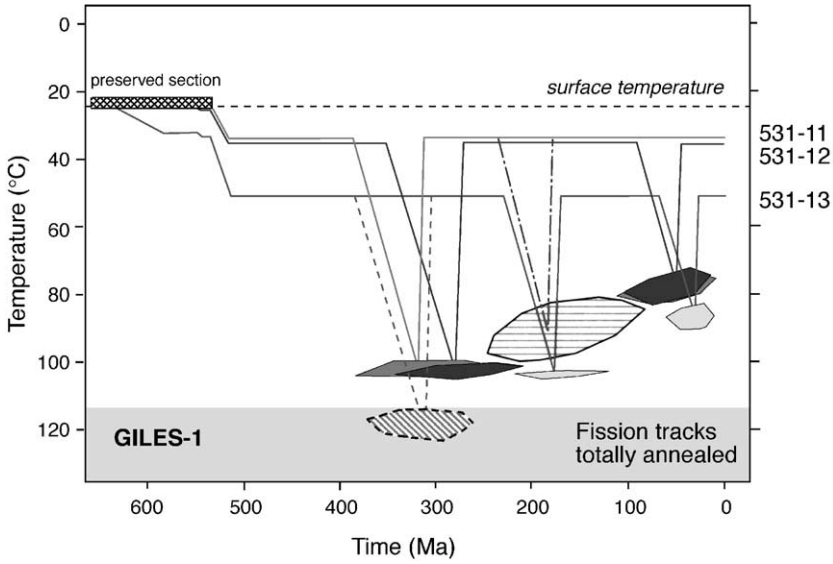

Fig. 7. AFTA thermal history solutions for the three samples from Giles-1. The shaded polygonal areas represent the ± 95% confidence limits on the two thermal episodes resolved in each sample. The horizontal-hatched area represents a thermal episode allowed by the results in samples 531-11 and 12, with cooling from paleotemperatures intermediate between those in the two defined episodes. Similarly, the crosshatched area depicts a notional event allowed by the results in sample 531-13, but which cannot be resolved due to the high paleotemperatures experienced more recently.

110 °C (325 to 200 Ma), sample GC531-6 from 100 to 110 °C (300 to 190 Ma), sample GC531-7 from >105 °C (270 to 200 Ma) and sample GC531-8 from 100 to 105 °C (310 to 160 Ma). Results from sample GC531-5 allow, but do not require, elevated paleotemperatures during this interval (Table 3; Fig. 8).

The similarity in paleotemperatures experienced by each sample (Table 3) for the overlapping time intervals suggests either that the thermal gradient was very low (Fig. 9), or that the effects of two different thermal episodes have not been resolved. For example, two events similar in timing to those revealed in Giles-1 would also be compatible with the Manya-2, Manya-5 and Manya-6 results; viz. 350 to 250 and 210 to 110 Ma.

Overlapping AFTA timing constraints also suggest a second consistent thermal episode, with cooling beginning between 70 and 15 Ma (Maastrichtian to mid-Miocene): sample GC531-3 from 75 to 90 °C, sample GC531-4 from 75 to 85 °C, sample GC531-6 from 75 to 85 °C, sample GC531-7 from 65 to 85 °C and sample GC531-8 from 75 to 85 °C.

At least one thermal episode is required by the AFTA data in the Permian samples (GC531-1 and -2) analysed from Manya-2, with cooling from 60 to 85 °C beginning at some time within the last 70 Ma. An earlier episode of cooling from 85 to 110 °C beginning between deposition (at ~ 280 Ma) and 80 Ma is allowed but not required. Results from the deeper Manya-2 samples indicate a thermal episode between the Early Permian and 200 Ma is also required.

4.4.4. Summary of AFTA thermal history constraints

In summary, the AFTA results alone reveal that the Cambrian and older sections were subjected to a number of pre- and post-Permian thermal episodes across the eastern Officer Basin. Results from all wells are consistent with a cooling from a thermal episode beginning at some time between the Maastrichtian and Miocene, 70 to 20 Ma (Fig. 8). AFTA results from Giles-1 indicate at least two pre-Cretaceous thermal episodes with the favoured interpretation of the overlapping timing constraints suggesting cooling beginning between 350 and 250 Ma (Carboniferous– Permian) and between 210 and 110 Ma (Late Triassic–Albian).

In Manya-2, -5 and -6 and Lake Maurice West-1, at least one earlier, higher temperature events is revealed

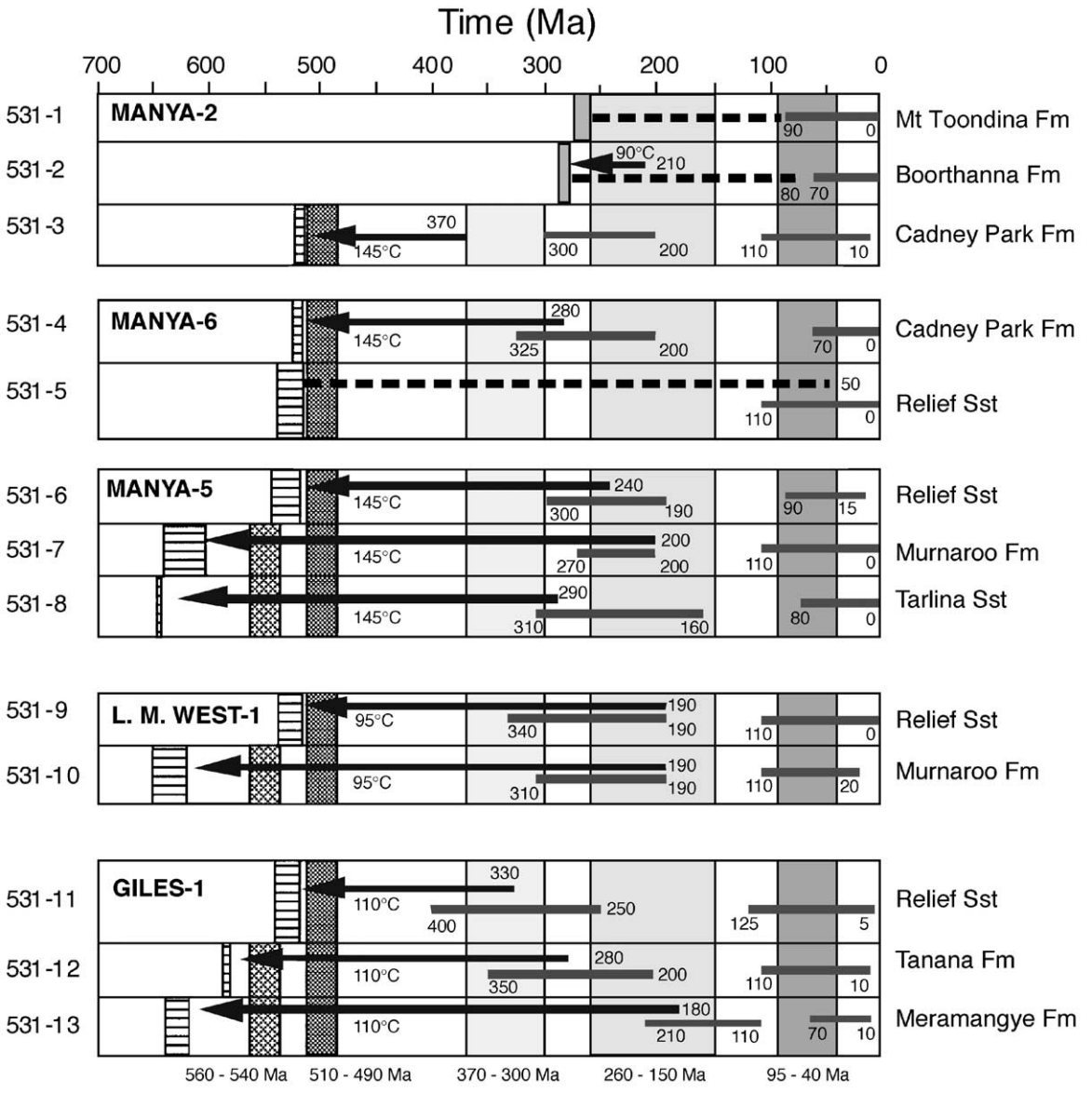

Fig. 8. Summary of AFTA-derived timing constraints for all well samples from the Officer Basin. The horizontal hatched boxes indicate the stratigraphic age constraints for each sample and the solid horizontal bars indicate the time range (95% confidence limits) of each thermal episode required by AFTA in that sample. Dashed horizontal bars mark thermal episodes, allowed, but not required, by AFTA. The left-pointing solid bars indicate the allowed timing range derived from AFTA for the maximum paleotemperatures (as indicated) derived from organic maturity data. For example, in sample 531-4 from Manya-6 a maximum paleotemperature of 145 °C, is only allowed by the AFTA results in the same unit prior to 280 Ma. The various shaded columns indicate time ranges (see text and Figs. 2 and 3) in which tectonic events are likely to have occurred (e.g. Hoskins and Lemon, 1995), or after 300 Ma, where no regional sedimentary record is currently preserved. These time ranges can be compared with the AFTA constraints.

with cooling beginning between 270 and 200 Ma (Late Permian to Late Triassic). The high paleotemperatures to which the analysed samples were subjected in the Late Permian to Late Triassic means that the AFTA data allows, but cannot resolve, even higher paleotemperatures in the period between Cambrian or

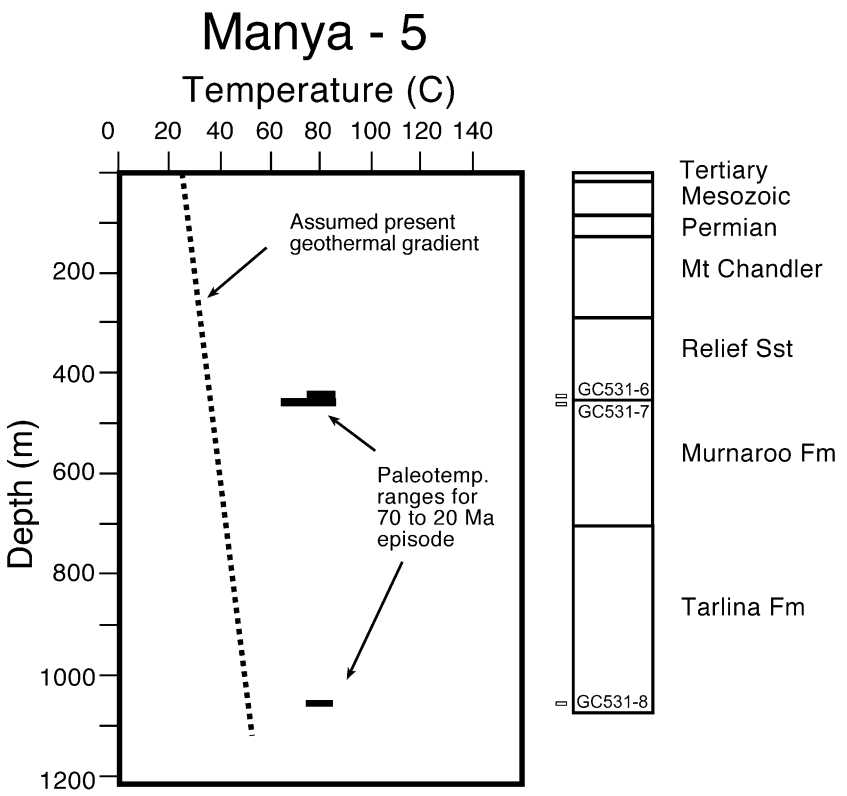

Fig. 9. Plot of AFTA derived paleotemperatures versus depth for the 70- to 20-Ma episode in Manya-5 (data from Table 4). The dashed line shown for comparison is the assumed present-day gradient of 25°/km.

Precambrian deposition and the recognised thermal episodes. Further insight into this aspect of the thermal history is obtained by integration with the organic maturity data discussed in a later section.

4.5. Estimation of paleogeothermal gradient and mechanisms of heating and cooling

Paleotemperature estimates over a range of depths for a given thermal episode revealed by AFTA can be used to constrain the paleogeothermal gradient for that particular time interval (Bray et al., 1992). In the wells studied here, paleotemperature profiles are generally defined by only two samples per well over a limited depth range, and therefore rigorous determination of paleogeothermal gradients is not possible. Furthermore, a number of the thermal episodes identified in the time interval prior to the Tertiary are represented by only single samples, with some evidence that multiple events may be unresolved within the overlapping time intervals interpreted from the AFTA results.

For these reasons, only the paleotemperature constraints obtained from the pervasive Maastrichtian–Miocene thermal episode (70 to 20 Ma) are used to provide some general information on the paleogeothermal gradient (e.g., Manya-5, Fig. 9). Table 4 shows calculated geothermal gradients for various wells. Calculations were only made for pairs of samples with depth differences of approximately 500 m or greater and with suitable paleotemperature data.

Mean gradients for the 70 to 20 Ma episode range between 16 and 0 °C/km but are not tightly constrained, with maximum allowed values ranging from ~ 17 to 33 °C/km (Table 4). These values are within the normal crustal range and are broadly consistent with the value of 25 °C/km assumed for the present-

day gradient. The limited vertical spread of results and the difficulty in resolving individual events in the low temperature part of the thermal history are the main reasons for the uncertainties in thermal gradient estimates. In general terms, paleogeothermal gradients of this level, when combined with the AFTA paleotemperature estimates for this episode (Table 3), suggest kilometre-scale erosion associated with cooling beginning between 70 and 20 Ma across the region. A more detailed treatment is not considered warranted at this stage.

While no effective paleogeothermal gradient constraints could be obtained for the earlier thermal episodes, subsequent cooling in each of these episodes is also interpreted to have been associated with kilometre-scale erosion for any reasonable paleogeothermal gradient. This conclusion does not preclude elevated basal heat flow as a mechanism of heating in these thermal episodes, but simply recognises that the magnitude of paleotemperatures revealed by AFTA in Paleozoic and Precambrian samples at present shallow depths necessitates kilometre-scale erosion when combined with any reasonable basal heat flow.

5. Integration of AFTA with organic maturity data

5.1. Organic maturity data

Organic maturity data are extremely sparse in the Officer Basin, primarily as a result of the age of the preserved stratigraphic section. Limited vitrinite reflectance and FAMM data are available from thin, and discontinuous Permo-Carboniferous sediments, while a small number of equivalent VR values (VRE) determined from methylphenanthrene index (MPI) values are available for a number of Cambrian and Proterozoic samples studied (Table 5). Maximum paleotemperatures have been estimated from these VR and VRE values using the EasyRo calculation (Burnham and Sweeney, 1989; Fig. 10).

5.2. Paleozoic and Neoproterozoic episodes

In Giles-1, AFTA indicates that the Early Cambrian and Neoproterozoic sections cooled from elevated temperatures of around 100 °C beginning between 350 and 250 Ma. A maximum paleotemperature of approximately 110 °C estimated from VRE values derived from the Neoproterozoic Alinya Formation (Table 5) is similar to the maximum temperature estimated from AFTA in related samples, suggesting that AFTA does record the time of maximum paleotemperatures. The Carboniferous–Permian time of cooling of this episode (350 to 250 Ma) is consistent with uplift and erosion in the Alice Springs Orogeny as has been observed in the Amadeus Basin to the north (Wells et al., 1970; Shaw, 1991; Tingate, 1990). Thus, the timing of peak hydrocarbon source rock maturation for the Cambrian and Neoproterozoic sections in Giles-1 is considered likely to have occurred during the Alice Springs Orogeny, although earlier maturation cannot be ruled out. Fig. 10 provides a schematic thermal history for the Giles-1 area derived from the available constraints.

In Manya-6, VRE results indicate that the Cambrian Ouldburra Formation has been heated to a maximum paleotemperature of approximately 145 °C at some time after deposition (Table 5). Applying this constraint to the AFTA results from Cambrian sample

Table 4
Paleogeothermal gradients for the 70- to 20-Ma AFTA episode

Well	Sample	Depth (m)	T_{max} (°C)	T_{min} (°C)	Mean gradient (°C/km)	Min. gradient (°C/km)	Max. gradient (°C/km)
Manya-5	531-6	455	85	75	0	− 16.7	16.7
	531-7	457	85	65	8.4	− 16.7	33.4
	531-8	1055	85	75			
Manya-6	531-4	449	85	75			24
	531-5	1700	< 105				
Giles-1	531-11	417	85	75	11.7	0	23.4
	531-12	423	85	70	15.7	0	31.3
	531-13	1064	90	85			

Table 5
Vitrinite reflectance and vitrinite reflectance equivalent (VRE) data for the eastern Officer Basin (McKirdy and Michaelsen, 1994; Kamali, 1995; Keiraville Konsultants, 1994; Michaelsen et al., 1997)

Depth (m)	Sample type	Formation	$R_v$max (%)	N	MPI	VRE (%)[a]	TM (°C)[b]	Analyst comment
Manya-2								
255.3	core	Mt Toondina Fm	0.40	25			65	
267.0	core	Mt Toondina Fm	0.35	25			55	suppressed
267.3	core	Mt Toondina Fm	0.38	15			65	
267.3	core	Mt Toondina Fm				0.54[c]	90	
444.9	core	Boorthanna Fm	0.51	2			85	
496.5	core	Boorthanna Fm	0.45	2			75	
Manya-6								
698.6	core extract	Ouldburra Fm			1.11	1.07	145	
Lake Maurice West-1								
417.7	core extract	Dey Dey Mudstone			0.28	0.57	95	
418.2	core extract	Dey Dey Mudstone			0.29	0.57	95	
Giles-1								
1237.0	core extract	Alinya Fm			0.43	0.66	110	

[a] Vitrinite reflectance equivalent (VRE) calculated from methylphenanthrene index (MPI).
[b] TM is maximum paleotemperature indicated by $R_v$max or VRE values using EasyRo (Burnham and Sweeney, 1989) with a heating rate of 1 °C/Ma and a cooling rate of 10 °C/Ma.
[c] VRE derived from fluorescence alteration of multiple macerals (FAMM) (Wilkins et al, 1994).

GC531-4 in Manya-6 suggests that this section must have reached maximum paleotemperatures prior to the 325 to 200 Ma AFTA episode in this sample which only involved paleotemperatures of 105 to 110 °C (Table 3). However, remodeling the AFTA data shows that the VRE-derived maximum paleotemperature of 145 °C may have occurred at any time between Cambrian deposition and approximately 280 Ma in sample GC531-4, as shown by the constraints in Fig. 8. If this maximum paleotemperature is used as a constraint on all of the Manya well samples, then all AFTA results would be consistent with cooling from 145 °C at any time prior to 290 Ma (Fig. 8). It is difficult to ascribe a more precise timing to the maximum paleotemperature event in the Manya wells, but on geologic grounds it probably occurred prior to exhumation and erosion during either the Delamerian (510–490 Ma) or Alice Springs Orogenies (370–300 Ma) which are known to have affected the broader region. A schematic thermal history for the Manya area drawn from all available constraints is shown in Fig. 10.

VRE values in Lake Maurice West-1 suggest a maximum paleotemperature for the Neoproterozoic of approximately 95 °C (Table 5), which is a little lower than the paleotemperature of 100 to 105 °C required between 310 and 190 Ma by AFTA data for the slightly deeper Neoproterozoic sample GC531-10 (Table 3). On balance, it is likely that peak source rock maturation in Lake Maurice West-1 occurred during this episode recorded by AFTA, and was associated with the final stages of the Alice Springs Orogeny (370 to 300 Ma), although a time as young as 190 Ma is possible.

5.3. Permian–Triassic episodes

AFTA data from Manya-2, -5 and -6 and Lake Maurice West-1 show consistent evidence of cooling from elevated temperatures beginning between 270 and 200 Ma, after deposition of the Permian section preserved in the Manya-2 well (Fig. 8). The AFTA-derived thermal history of sample GC531-4 from Manya-6 illustrates this event (Fig. 10). Also shown in Fig. 10 are maximum paleotemperature constraints from vitrinite reflectance data (Table 5) from the shallower Permian units in Manya-2 (Keiraville Konsultants, 1994), and the AFTA thermal history constraints from Permian sample GC531-2 in the same well. VR levels vary from 0.35 to 0.51 ($R_v$max), but

an associated FAMM VRE of 0.54% and organic petrology observations (Keiraville Konsultants, 1994) further suggest that the lower reflectance values are likely to be geochemically suppressed, and the higher values that give a maximum paleotemperature of 90 °C (Table 5) are considered the most reliable indicators of thermal maturity. Combining this constraint with the AFTA data in sample GC531-2, suggests that a max-

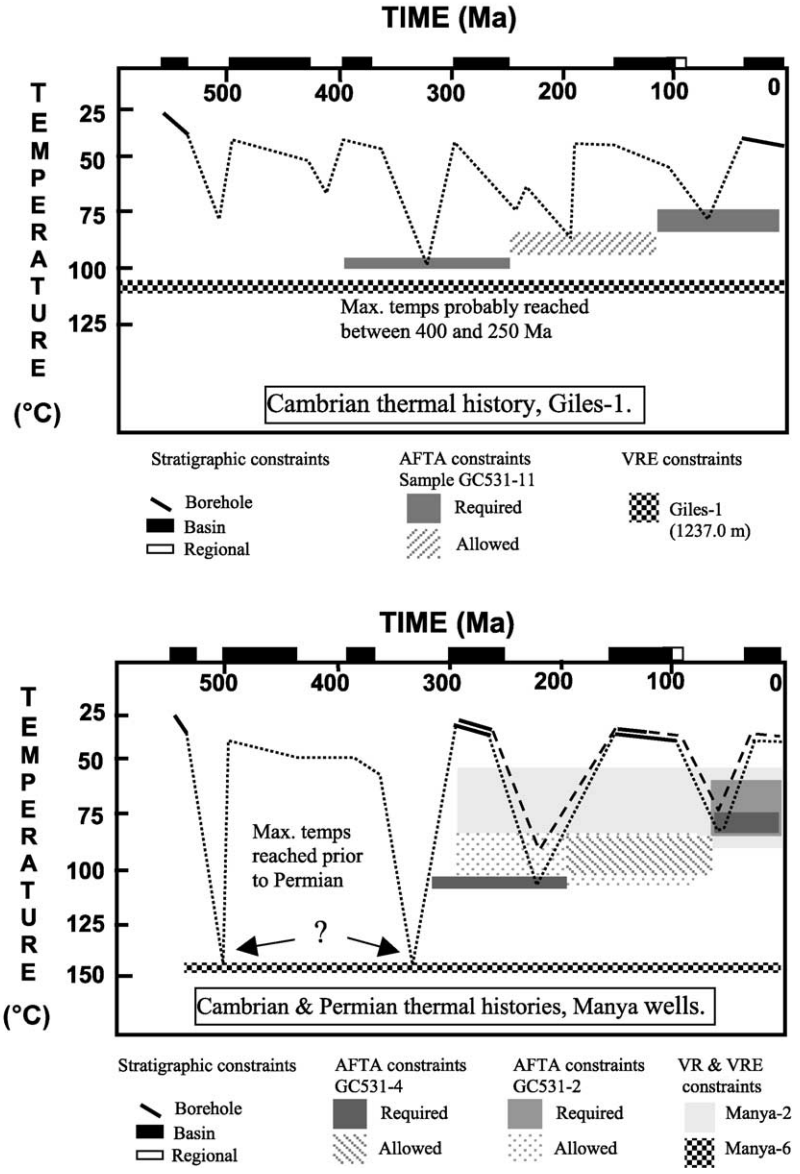

Fig. 10. Schematic illustration of the regional thermal history of the Officer Basin established in this study based on for AFTA thermal history solution for samples GC531-2 (Manya-2), GC531-4 (Manya-6) and GC531-11 (Giles-1) together stratigraphic and organic thermal maturity constraints (Tables 3 and 5; Fig. 8). The dashed lines indicate possible thermal histories for selected horizons in each well linked to successive periods of heating associated with burial, and cooling associated with erosion. Borehole stratigraphic constraints refer to stratigraphy preserved within the borehole; basin constraints refer to the maximum extent of preserved sedimentation within the eastern Officer Basin; and regional constraints refer to the preserved stratigraphy in the neighbouring regions.

imum paleotemperature of 90 °C could only have occurred between Permian deposition and 210 Ma (Fig. 8), consistent with the 270 to 200 Ma episode defined by the AFTA results in the older section.

6. Regional geological considerations

6.1. Early cretaceous to late tertiary events

Fig. 10 illustrates the time and temperature conditions that satisfy the AFTA results in one sample from Giles-1 (GC531-11) and two samples from the Manya-2 and -6 wells, GC531-2 and GC531-4, respectively. Available stratigraphic constraints derived from each well, regional information and other thermal maturity indicators are also shown. In the case of the post-Albian AFTA episode(s), the overlapping AFTA timing constraints obtained from all samples (70 to 20 Ma) is assumed to apply in all of the wells studied. This Late Cretaceous–Tertiary cooling episode in the Officer Basin appears to be part of a larger regional pattern of cooling recognised by other fission track studies (Fig. 11). Areas exhibiting cooling at similar times include the southern Arunta and northern Musgrave Blocks and Amadeus Basin (Tingate, 1990), the western margin of the Eromanga Basin (Tingate and Duddy, 1996) and the Adelaide Fold Belt (Mitchell et al., 1998; Foster et al., 1994; Gibson and Stuwe, 2000).

The youngest deposits in the study area are scattered, unconsolidated, paleochannel deposits of the late Middle Eocene–Pliocene Immarna Group (Benbow et al., 1995) which occur in the southern part of the Officer Basin. The presence and unconsolidated nature of these Tertiary deposits suggests that little of the regional erosion associated with this cooling episode occurred after 40 Ma.

No definite mid-Cretaceous thermal episode is defined by the overlap of AFTA timing constraints in all samples for the wells studied. However, results in most samples could accommodate a thermal episode from which cooling began between 110 and 70 Ma (Fig. 8), and this would be consistent with a regional unconformity separating the Early Cretaceous Bulldog Shale of the Mesozoic Eromanga Basin succession (Krieg et al., 1995) from thin Tertiary sands, spanning the time interval 95 to 40 Ma (Fig. 8).

The elevated paleotemperatures recorded by AFTA for this time interval are consistent with a greater depth of burial followed by erosion, but the lack of rigorous estimates of paleogeothermal gradient precludes accurate estimates of former burial depths prior to cooling beginning between 95 and 40 Ma. A general estimate can be made using the paleotemperature estimates for each sample given in Table 3, assuming a paleo-surface temperature of 25 °C and a paleogeothermal gradient of 25 °C/km. On this basis, the Paleozoic and Proterozoic rocks now at outcrop in the Officer Basin are estimated to have undergone around 1 to 2 km of erosion between 95 and 40 Ma.

In the Poolowanna Trough, 500 km north–west of the study area, the maximum preserved thickness of Bulldog Shale and overlying Cretaceous formations is approximately 2 km, including 1 km of Albian–Cenomanian Winton Formation (Moore and Pitt, 1982). The Winton Formation is the youngest formation in the Eromanga Basin and has a depositional age range of 97–90 Ma (Krieg et al., 1995). Burial of this age and magnitude could explain the elevated post-Early Cretaceous paleotemperatures derived from the AFTA data, for cooling beginning at any time since 90 Ma. Some additional support for this magnitude of erosion come from the degree of gellification of telovitrinite in the Permian Mt Toondina Formation in Manya-2 which suggests a maximum depth of burial at least 1 km greater than the present burial depth (Keiraville Konsultants, 1994).

Combining the AFTA and stratigraphic constraints, it is likely that an originally thicker and more extensive equivalent succession to the Eromanga Basin sequence was present over much of the eastern Officer Basin, and this was eroded between 70 and 40 Ma, although erosion starting as young as 110 Ma would be allowed by much of the AFTA data.

6.2. Permian–Triassic events

A 270- to 200-Ma thermal episode is revealed by AFTA in most of the Officer Basin wells studied. Assuming that additional burial is the major cause of heating in the 270 to 200 Ma episode, the AFTA time constraints suggest that a greater thickness of Permian and/or Triassic strata was once present in the basin. Within the basin, the youngest preserved Permian unit is the Mt Toondina Formation, which ranges in age

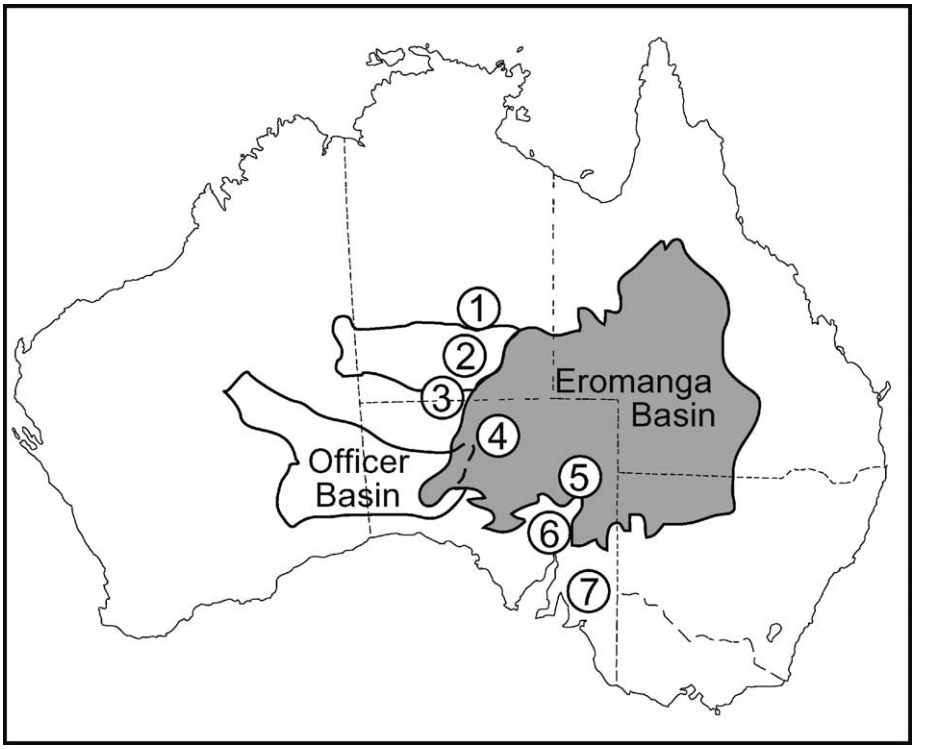

Fig. 11. Map showing regions with fission track thermal history constraints referred to in the text: (1) Arunta Block, (2) Amadeus Basin and (3) Musgrave Block (Tingate, 1990), (4) western Eromanga Basin (Tingate and Duddy, 1996), (5) northern Flinders Ranges (Foster et al., 1994), (6) Flinders Ranges (Mitchell, 1998) and (7) Adelaide Hills (Gibson and Stuwe, 2000).

from 270 to 260 Ma. If the observed paleotemperatures were caused by greater burial then the time range over which elevated paleotemperatures could have occurred can be further constrained to between 260 and 200 Ma by using the AFTA constraints. Estimates of the magnitude of former burial prior from paleotemperatures experienced prior to cooling beginning between 270 and 200 Ma range from approximately 2 to 3 km assuming a paleo-surface temperature of 25 °C and a paleogeothermal gradient of 25 °C/km. Without constrained paleogeothermal gradients, any estimates of eroded section should be treated only as indications of the magnitude of erosion.

The Permian deposits that overlie the Officer Basin are part of the Arckaringa Basin succession which has a maximum preserved thickness of 1 km approximately 150 km west of the Officer Basin. The top of this succession has vitrinite reflectance values around 0.5% which suggests that the preserved succession is itself likely to be a remnant of a once thicker section (Moore, 1982).

An episode of similar age and magnitude has been identified from apatite fission track results by Tingate (1990) in the Amadeus Basin, Arunta Block and the northern part of the Musgrave Block (Fig. 11). AFTA results from one shallow Cambrian sample from near the western margin of the Eromanga Basin (Fig. 11) reported a paleotemperature of 60–90 °C prior to cooling, beginning between 300 and 100 Ma (Tingate and Duddy, 1996).

6.3. Paleozoic events

It has not been possible to determine the geothermal gradients acting during any of the pre-Late Cretaceous thermal episodes revealed by AFTA. In general, however, maximum temperatures during the Paleozoic episodes are around 100 °C (Table 3) and therefore for any range of geologically reasonable

geothermal gradients, kilometre-scale erosion is required.

In Giles-1, the cooling beginning between 350 and 250 Ma is considered likely to be associated with the Alice Springs Orogeny (Figs. 2 and 3). There is evidence of this event in regions adjoining the study area with more precise timing constraints. Late Devonian–Carboniferous deformation and erosion in the Amadeus Basin and Arunta and Musgrave Blocks occurred as part of the Alice Springs Orogeny (Forman, 1966). K–Ar and Rb–Sr isotopic mineral ages suggest that the main phase of compressional deformation occurred between 330 and 310 Ma (Shaw et al., 1984). Fission track data in the region are also consistent with a cooling event at this time (Tingate, 1990). Fission track data from the Mesoproterozoic Musgrave Block and Cambrian sedimentary rocks near the western margin of the Eromanga Basin also show evidence of cooling from temperatures greater than 100 °C starting between 360 and 300 Ma (Tingate and Duddy, 1996). Cooling of similar age and magnitude has also been reported further south in the Adelaide Fold Belt (Mitchell et al., 1998; Foster et al., 1994; Gibson and Stuwe, 2000).

7. Implications for hydrocarbon exploration

The regional distribution of published Neoproterozoic, Cambrian and Devonian VRE values derived from methylphenanthrene index (MPI) data (Gravestock and Hill, 1997) are shown in Fig. 12. The VRE values vary from 1.7% to 0.57%, generally decreasing to the southwest, a trend which is not related to present depth or temperature. Maturity levels greater than 1.0% are associated with regions which experienced or were proximal to active thrusting during the Neoproterozoic or Paleozoic (Gravestock and Hill, 1997). In general, the Neoproterozoic sedimentary rocks have similar or lower VRE values than the Cambrian samples (Fig. 12), suggesting that the timing of maximum paleotemperatures is Cambrian or younger. In Fig. 12, locally low Neoproterozoic VRE values (e.g., Observatory Hill-1) do not occur in wells with high Cambrian values and appear to reflect local variability in the thermal history of the region. The presence of Neoproterozoic-sourced oil in Cambrian sandstones in Observatory Hill-1 (Gravestock and Hill, 1997) also supports this timing constraint. In Munyarai-1 similar high VRE values from Neoproterozoic and Devonian samples (Fig. 12) suggest maximum paleotemperatures occurred, at least locally, post-Devonian. However, no other VRE data exist for the post-Cambrian section in the basin.

The thermal history interpreted from the AFTA data demonstrates the presence of major thermal episodes significantly younger than the youngest deformational event recognised in the basin, the Alice Springs Orogeny (370 to 300 Ma). Near the northeastern margin of the basin in Manya-2, -5 and -6, the AFTA data indicate that the Permian, Cambrian and Neoproterozoic section cooled from high paleotemperatures in at least two events between 270 and 200 Ma and again between 70 and 15 Ma. The AFTA data are consistent with earlier higher temperature events (>145 °C) indicated by a VRE values in the Manya-6. Therefore, peak maturation in these wells is likely to have been associated with either the Alice Springs or Delamerian Orogenies.

In Giles-1, the similarity of maximum paleotemperatures derived from AFTA and VRE strongly suggest that peak maturation occurred prior to the Permian. The timing constraints are not very precise but peak maturation probably occurred during the Alice Springs Orogeny. Further southwest in Lake Maurice West 1, the maximum paleotemperatures indicated by AFTA are slightly higher than those estimated from Neoproterozoic VRE values and peak maturation therefore occurred prior to the latest Triassic.

Significantly, the reconstructed thermal histories do not preclude relatively young source rock maturation in the Officer Basin. The identification of elevated temperatures in the Devonian to Triassic in Giles-1 and Lake Maurice West-1 tends to upgrade petroleum prospectivity as any hydrocarbon accumulation generated does not necessarily have to occur early in the history of the basin (Late Neoproterozoic to Late Cambrian, depending on the age of the source interval). If peak maturation occurred later, there is greater chance of preservation of accumulations as they would not have experienced as many deformation episodes since emplacement. The Amadeus Basin to the north of the Officer Basin has economic accumulations with a similar style of thermal history to the Officer Basin (Tingate, 1990). Peak maturation of

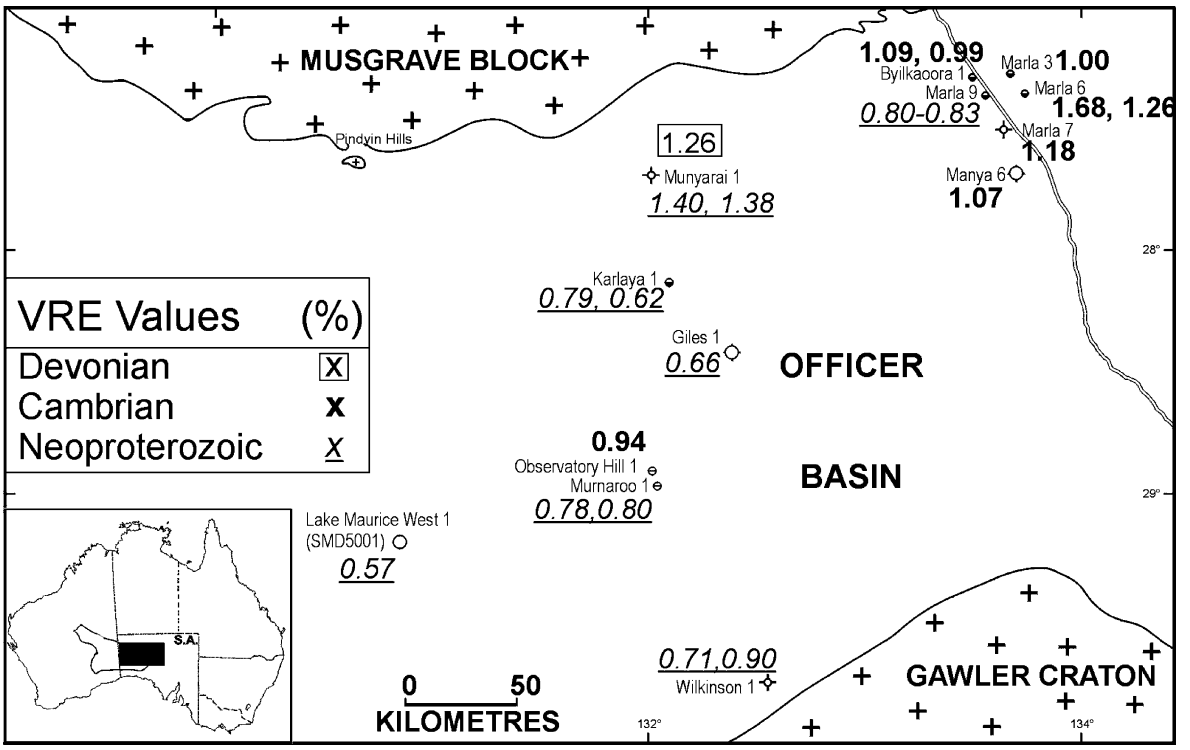

Fig. 12. Maturity (vitrinite reflectance equivalent %) map derived from MPI data for Devonian, Cambrian and Neoproterozoic rocks in the eastern Officer Basin.

source rocks associated with the Palm Valley Gas Field and Mereenie Oil Field probably occurred prior to cooling starting between 240 and 170 Ma (Tingate, 1990). The AFTA data also indicate that the thin Permian and Mesozoic successions overlying the Officer Basin are themselves early mature.

8. Conclusions

Integration of the AFTA fission track results and limited organic maturity data has revealed that at least three and possibly more, regional thermal episodes have affect the Officer Basin sequence between the Devonian and the present day. All of the events must have involved kilometre-scale erosion even allowing for the possibility of elevated basal heat flow associated with some episodes.

The study demonstrates the unique ability of AFTA fission track results in constraining the thermal, burial and hydrocarbon maturity history of old basins where conventional technologies cannot be applied. Integration with organic maturity data, including MPI data, provides further insights into the thermal and hydrocarbon maturation histories not available from either technique when used in isolation. In particular, thermal history reconstruction has allowed ranking of previously recognised tectonic events in terms of their thermal importance, but has also revealed younger thermal events that have a significant impact on hydrocarbon prospectivity.

Finally, the thermal history of the Officer Basin has not been completely resolved but the importance of younger thermal episodes, apparently related to tectonic events better preserved in the geological histories of neighbouring basins, has been clearly revealed. The possibility of younger thermal events affecting ancient sedimentary basins is not surprising in itself, but until recognised it is natural for workers in ancient basins to tend to stress the importance of geological events recorded in the preserved sedimentary record, even though such early events may not be the major

control on the thermal history or timing of peak maturation.

Acknowledgements

The authors would like to acknowledge the Petroleum Group from Primary Industries and Resources South Australia (PIRSA) for originally supporting the AFTA study and supplying electronic versions of some figures. We would also like to acknowledge, in particular, the late Dr. David Gravestock of PIRSA for his helpful discussions and enthusiasm for new initiatives in the Officer Basin. The authors gratefully acknowledge Geotrack International for its support of this study and use of facilities to reanalyse samples. Peter Tingate acknowledges support from the Australian Petroleum Cooperative Research Centre (APCRC). AFTA® is a registered trademark of Geotrack International. The authors thank Shimon Feinstein, Malcolm Wallace and Annette George for their constructive reviews.

References

Benbow, M.C., Lindsay, J.M., Alley, N.F., 1995. Eucla Basin and Palaeodrainage. In: Drexel, J.F., Preiss, W.V. (Eds.), The Geology of South Australia: Vol. 2. The Phanerozoic. S.A. Geol. Surv. Bull., vol. 54, pp. 178–186.

Bray, R., Green, P.F., Duddy, I.R., 1992. Thermal history reconstruction in sedimentary basins using apatite fission track analysis and vitrinite reflectance: a case study from the East Midlands of England and the Southern North Sea. In: Hardman, R.F.P. (Ed.), Exploration Britain: Into the Next Decade. Geological Society London, Special Publication, vol. 67, pp. 3–25.

Burnham, A.K., Sweeney, J.J., 1989. A chemical kinetic model of vitrinite maturation and reflectance. AAPG Bull. 74 (10), 1559–1570.

Duddy, I.R., Green, P.F., Laslett, G.M., 1988. Thermal annealing of fission-tracks in apatite: III. Variable temperature behaviour. Chem. Geol. (Isot. Geosci. Sect.) 73, 25–38.

Forman, D.J., 1966. Regional Geology of the South West Margin of the Amadeus Basin, Central Australia. Bureau of Mineral Resources, Australia Report 87.

Foster, D.A., Murphy, J.M., Gleadow, A.J.W., 1994. Middle Tertiary hydrothermal activity and uplift of the northern Flinders Ranges, South Australia: insights from apatite fission track thermochronology. Aust. J. Earth Sci. 41, 11–17.

Galbraith, R.F., 1990. The Radial plot: graphical assessment of spread in ages. Nucl. Tracks Radiat. Meas. 3, 207–214.

Geotrack, 1994. Apatite fission track analysis of fourteen well samples. Geotrack Report #531 (unpublished report prepared for Mines and Energy, South Australia).

Gibson, H.J., Stuwe, K., 2000. Multiphase cooling and exhumation of the southern Adelaide Fold Belt: constraints from apatite fission track data. Basin Res. 12, 31–45.

Gleadow, A.J.W., Duddy, I.R., Lovering, J.F., 1983. Fission track analysis: a new tool for the evaluation of thermal histories and hydrocarbon potential. APEA J. 23, 93–102.

Gleadow, A.J.W., Duddy, I.R., Green, P.F., Lovering, J.F., 1986. Confined fission track lengths in apatite—a diagnostic tool for thermal history analysis. Contrib. Mineral. Petrol. 94, 405–415.

Gravestock, D.I., 1997. Geological setting and structural history. In: Morton, J.G.G., Drexel, J.F. (Eds.), Petroleum Geology of South Australia, vol. 3. Officer Basin. South Australian Department of Mines and Energy Resources (SADME) Report Book 97/19, pp. 5–44.

Gravestock, D.I., Hill, A.J., 1997. Petroleum maturation and migration. In: Morton, J.G.G., Drexel, J.F. (Eds.), Petroleum Geology of South Australia, vol. 3. Officer Basin. South Australian Department of Mines and Energy Resources (SADME) Report Book 97/19, pp. 109–120.

Gravestock, D.I., Morton, J.G.G., 1997. Source rock distribution and quality. In: Morton, J.G.G., Drexel, J.F. (Eds.), Petroleum Geology of South Australia, vol. 3. Officer Basin. South Australian Department of Mines and Energy Resources (SADME) Report Book 97/19, pp. 99–108.

Green, P.F., 1988. The relationship between track shortening and fission track reduction in apatite: combined influences of inherent instability, geometry, length bias and system calibration. Earth Planet. Sci. Lett. 89, 335–352.

Green, P.F., Duddy, I.R., Gleadow, A.J.W., Tingate, P.R., Laslett, G.M., 1985. Fission-track annealing in apatite: track length measurements and the form of the Arrhenius Plot. Nucl. Tracks 10 (3), 323–328.

Green, P.F., Duddy, I.R., Gleadow, A.J.W., Tingate, P.R., Laslett, G.M., 1986. Thermal annealing of fission tracks in apatite: 1. A qualitative description. Chem. Geol. (Isot. Geosci. Sect.) 59, 237–253.

Green, P.F., Duddy, I.R., Gleadow, A.J.W, Lovering, J.F., 1989a. Apatite fission track analysis as a paleotemperature indicator for hydrocarbon exploration. In: Naeser, N.D., McCulloch, T. (Eds.), Thermal History of Sedimentary Basins—Methods and Case Histories. Springer, New York, pp. 181–195.

Green, P.F., Duddy, I.R., Laslett, G.M., Hegarty, K.A., Gleadow, A.J.W., Lovering, J.F., 1989b. Thermal annealing of fission tracks in apatite: 4. Quantitative modelling techniques and extension to geological timescales. Chem. Geol. (Isot. Geosci. Sect.) 79, 155–182.

Green, P.F., Hegarty, K.A., Duddy, I.R., 1996. Compositional influences on fission track annealing in apatite an improvement in routine application of AFTA®. Am. Assoc. Pet. Geol. A56, San Diego Meeting, Abstracts with program.

Hoskins, D., Lemon, N.M., 1995. Tectonic development of the eastern Officer Basin, central Australia. Explor. Geophys. 26, 395–402.

Kamali, M.R., 1995. Petroleum geochemistry of Early Cambrian carbonate source rocks, Ouldburra Formation, eastern Officer

Basin. Report submitted to South Australian Department of Mines and Energy. Open file envelope, 8591 (unpublished).

Keiraville Konsultants, 1994. Organic petrographic report on samples from Manya-2, Middle Bore-1, Mt Willoughby-1. Keiraville Konsultants; 5 pp. Unpublished report submitted to Mines and Energy South Australia.

Krieg, G.W., Alexander, E.M., Rogers, P.A., 1995. Jurassic Cretaceous Epicratonic Basins. In: Drexel, J.F., Preiss, W.V. (Eds.), The Geology of South Australia: Vol. 2. The Phanerozoic. Geol. Surv. Bull., vol. 54, pp. 101–123.

Laslett, G.M., Gleadow, A.J.W., Duddy, I.R., 1984. The relationship between fission track length and density in apatite. Nucl. Tracks 9, 29–38.

Laslett, G.M., Green, P.F., Duddy, I.R., Gleadow, A.J.W., 1987. Thermal annealing of fission-tracks in apatite: 2. A quantitative analysis. Chem. Geol. (Isot. Geosci. Sect.) 65, 1–13.

Lindsay, J.F., Leven, J.H., 1996. Evolution of a Neoproterozoic to Palaeozoic intracratonic setting, Officer Basin, South Australia. Basin Res. 8, 403–424.

Magoon, L.B., Dow, W.G., 1994. Ch. 1: the petroleum system. In: Magoon, L.B., Dow, W.G. (Eds.), The Petroleum System—From Source to Trap. AAPG Mem., vol. 60, pp. 3–24.

McKirdy, D.M., Michaelsen, B.H., 1994. Geochemical measurement of thermal maturity in Neoproterozoic and Cambrian sediments, eastern Officer Basin. Organic Geochemistry in Basin Analysis Group unpublished report submitted to South Australian Department of Mines and Energy, 8 pp.

McKirdy, D.M., Kantsler, A.J., Emmett, J.K., Aldridge, A.K., 1984. Hydrocarbon genesis and organic facies in Cambrian carbonates of the eastern Officer Basin, South Australia. In: Palacas, J.G. (Ed.), Petroleum Geochemistry and Source Rock Potential of Carbonate Rocks. AAPG Stud. Geol., vol. 18, pp. 13–31.

Michaelsen, B.R., Sherwood, N., McKirdy, D.M., Faiz, M.M., Watson, B.L., Whythe, S.R., 1997. Estimation of vitrinite reflectance suppression in potential hydrocarbon source rocks from the Pedirka, Arckaringa and western Eromanga Basins by FAMM. Unpublished report to Mines and Energy South Australia by University of Adelaide/CSIRO Petroleum/AMDEL Petroleum Services, p. 11.

Mitchell, M.M., 1998. Identification of multiple detrital source modes for Otway Super Group sedimentary rocks: implications for basin models and chronstratigraphic correlations. Aust. J. Earth Sci. 44, 743–750.

Mitchell, M.M., Kohn, B.P., Foster, D.A., 1998. Post-orogenic cooling history of eastern South Australia from Apatite Fission Track Thermochronology. In: Van Den Haute, P., De Corte, F. (Eds.), Advances in Fission Track Geochronology. Kluwer Academic Publishing, The Netherlands, pp. 207–224.

Moore, P.S., 1982. Hydrocarbon potential of the Arckaringa region, central South Australia. APEA J. 122, 237–253.

Moore, P.S., Pitt, G.M., 1982. Cretaceous of the southwestern Eromanga Basin: stratigraphy, facies variation and petroleum potential. In: Moore, P.S, Mount, T.J. (Compilers) Eromanga Basin Symposium summary papers. Geological Society of Australia and Petroleum Exploration Society of Australia, Adelaide, pp. 127–144.

Morton, J.G.G., 1997. Lithostratigraphy and environments of deposition. In: Morton, J.G.G., Drexel, J.F. (Eds.), Petroleum Geology of South Australia, vol. 3, pp. 47–86, Officer Basin, SADME Report Book 97/19.

Moussavi-Harami, R., Gravestock, D.I., 1995. Burial history of the eastern Officer Basin, South Australia. APEA J. 35 (1), 307–320.

O'Neil, B.J., 1997. History of petroleum exploration. In: Morton, J.G.G., Drexel, J.F. (Eds.), Petroleum Geology of South Australia, vol. 3. Officer Basin. South Australian Department of Mines and Energy Resources (SADME) Report Book 97/19, pp. 7–22.

Radke, M., Welte, D.H., 1983. The methylphenanthrene index (MPI): a maturity parameter based on aromatic hydrocarbons. In: Bjoroy, M. et al., (Eds.), Advances in Organic Geochemistry 1981. Wiley, Chichester, pp. 504–512.

Shaw, R.D., 1991. The tectonic development of the Amadeus Basin, central Australia. Bur. Miner. Resour., Geol. Geophys., Bull. (Aust.) 236, 429–462.

Shaw, R.D., Stewart, A.J., Black, L.P., 1984. The Arunta Inlier: a complex ensialic mobile belt in central Australia: Part 2. Tectonic history. Aust. J. Earth Sci. 31, 457–484.

Sherwood, N., Russell, N., 1996. Thermal maturity indicators compared. 13th Aust. Geol. Conv., Canberra, Feb., 1996. Geol. Soc. Aust. Abstracts, vol. 41, pp. 389.

Sieber, K.G., 1986. Structure of the Lower Cretaceous Sediments—Fish Creek Area, Victoria—and the Compositional Variation in Apatites. Bsc Honours Thesis, University of Melbourne (unpublished).

Tingate, P.R., 1990. Apatite fission track studies from the Amadeus Basin, central Australia. PhD Thesis, University of Melbourne (unpublished).

Tingate, P.R., 1994. Interpretation of apatite fission track data from the Officer Basin. Report submitted to Mines and Energy South Australia, 15 pp. (unpublished).

Tingate, P.R., Duddy, I.R., 1996. The thermal history of the Eringa Trough and western Eromanga Basin. In: Alexander, E., Hibburt, J. (Eds.), The Petroleum Geology of South Australia, vol. 2. Eromanga Basin. South Australian Department of Mines and Energy Resources (SADME) Report/Book 96-20, pp. 111–123.

Tingate, P.R., Duddy, I.R., 2000. Fission track data from the Officer Basin, South Australia. In: Noble, W.P., O'Sullivan, P.B., Brown, R.W. (Eds.), 9th International Conf. on Fission Track Dating and Thermochronology. Geol. Soc. Aust. Abstracts Series, vol. 58, p. 317.

Walter, M.R., Veevers, J.J., Calver, C.R., Grey, K., 1995. Neoproterozoic stratigraphy of the Centralian Superbasin, Australia. In: Knoll, A.H., Walter, M.R. (Eds.), Neoproterozoic Stratigraphy and Earth History. Precambrian Research, vol. 73; pp. 1–4, 173–195.

Wells, A.T., Forman, D.J., Ranford, L.C., Cook, P.J., 1970. Geology of the Amadeus Basin, central Australia. Bur. Miner. Resour., Bull. (Aust.), 100.

Wilkins, R.W.T., Russell, M.V., Ellacott, N.J., 1994. Fluorescence alteration and thermal maturity modelling of Carnarvon Basin wells. In: Purcell, P.G., Purcell, R.R. (Eds.), The North West Shelf Australia: Proceedings of PESA symposium, Perth, pp. 115–128.